

FE Implementation of Viscoelastic Constitutive Stress-Strain Relations Involving Fractional Time Derivatives

André Schmidt, Lothar Gaul

Institut A für Mechanik, Universität Stuttgart, Germany

ABSTRACT: Viscoelastic material behavior implies the capability to store a portion of its deformation energy whereas the remaining portion is dissipated, so called material damping. The damping properties of a structure may be modeled locally or globally using differential operators or hereditary integral viscoelastic constitutive equations.

Rheological damping models consisting of springs and dashpots result in constitutive stress-strain relations of differential operator type. They are known to have deficiencies when being applied to a broad range of time or frequencies. These drawbacks can only be minimized by using a large number of material parameters. Improved adaptivity with respect to measured constitutive behavior is obtained by the differential operator concept including fractional derivatives, where the theory of fractional derivatives can be considered as an extension of derivatives of integer order. This generalization to any real-order derivative results in non-local operators. Material models involving fractional time derivatives provide good curve-fitting properties, require only few parameters and lead to causal behavior. In addition, the concept of fractional derivatives in conjunction with viscoelastic constitutive equations is physically justified.

The implementation of fractional constitutive equations based on the Grünwaldian formulation into an elastic FE code is demonstrated. Parameter identifications for the fractional 3-parameter model in the time domain as well as in the frequency domain are carried out. The identified material model is used to perform an FE analysis of a viscoelastic structure.

1 INTRODUCTION

The history of fractional derivatives can be dated back to 1695, when L'Hospital and Leibniz were communicating whether it made sense to define an operator $\frac{d^n}{dt^n}$ for $n = 1/2$ (Leibniz 1962).

In the 18th century there were only few contributions to this topic and it was Euler who again raised the question of a derivative of order n for n being a fraction. In 1819 Lacroix first mentioned derivatives of arbitrary order in a text (Lacroix 1819). The first application of fractional derivatives was given in 1823 by Abel who applied the fractional calculus in the solution of an integral equation that arises in the formulation of the tautochrone problem (Abel 1881). Later, Liouville attempted to give a logical definition of fractional derivatives (Liouville 1832a, b, 1834).

One can state that the whole theory of fractional derivatives and integrals was established in the 2nd half of the 19th century. Further names to be mentioned are Grünwald, Krug, Riemann, and Letnikov. A more detailed overview concerning the history of fractional derivatives in general is given by Ross

(1975).

However, the term 'fractional' integrodifferential operators is misleading as it implies that only rational numbers as orders of derivatives or integrals are defined. In fact, the order of derivatives or integrals may be any real number; even for complex numbers fractional derivatives are defined.

In 1921 Nutting observed that stress relaxation of some materials might be modeled by fractional powers of time (Nutting 1921) and Gemant stated that the stiffness and damping properties of viscoelastic materials are fit much better by using fractional powers of frequency. The latter was the first who suggested explicitly to use fractional derivatives in the constitutive equation (Gemant 1936, 1938). Scott-Blair & Caffyn (1949) again suggested the application of fractional time-derivatives to meet the observations of Nutting and Gemant. Caputo and Mainardi (Caputo & Mainardi 1971a, Caputo 1974) also found good agreement with experimental results when using fractional derivatives for the description of viscoelastic materials and established the connection between fractional derivatives and the theory of linear

viscoelasticity (Caputo & Mainardi 1971b). Up to the beginning of the 80s, the concept of fractional derivatives in conjunction with viscoelasticity had to be seen as a sort of curve-fitting method. Then, Bagley & Torvik (1983) gave a physical justification for this concept. Starting point is the molecular theory of Rouse (1953), later modified by Ferry, Landel & Williams (1955), resulting in fractional derivatives of order 1/2 in the shear stress-strain relation. Similar considerations for the molecular theory of Zimm (1956) lead to a fractional derivative of order 2/3. As an example, Bagley & Torvik (1984) derived the equation of motion of a plate which is immersed into a Newtonian fluid and connected by a spring to a fixed point. The resulting damping force is found to be proportional to the fractional time derivative of the displacement of order 3/2.

Bagley & Torvik also developed constraints for the fractional 3-parameter model, ensuring the model to predict a non-negative rate of energy dissipation and internal work (Bagley & Torvik 1986).

The implementation of fractional constitutive equations into FE formulations was studied substantially by Padovan (1987). An application to a three dimensional structure is given by Schmidt, Oexl & Gaul (2000). Implementations into the BEM were investigated by Gaul & Schanz (1999) for the time domain and by Gaul (1999) for the frequency domain, respectively.

2 GRÜNWARD DEFINITION OF FRACTIONAL DERIVATIVES

There are different definitions of fractional derivatives. Best known are the Riemann-Liouville and the Grünwald definition which can be transformed into one another. However, the Grünwald definition involves the fewest restrictions on the functions to which it is applied and can be implemented easily into numerical algorithms.

Starting point is the definition of the first (integer order) time derivative in terms of a backward difference quotient

$$\frac{d^1 f(t)}{dt^1} = \lim_{\Delta t \rightarrow 0} \frac{1}{\Delta t} [f(t) - f(t - \Delta t)] \quad (1)$$

Repeated application leads to

$$\begin{aligned} \frac{d^2 f(t)}{dt^2} &= \lim_{\Delta t \rightarrow 0} \frac{1}{(\Delta t)^2} [f(t) - 2f(t - \Delta t) \\ &\quad + f(t - 2\Delta t)] \quad (2) \end{aligned}$$

$$\begin{aligned} \frac{d^3 f(t)}{dt^3} &= \lim_{\Delta t \rightarrow 0} \frac{1}{(\Delta t)^3} [f(t) - 3f(t - \Delta t) \\ &\quad + 3f(t - 2\Delta t) - f(t - 3\Delta t)] \quad (3) \end{aligned}$$

⋮

that can be written for any integer-order derivative as

$$\frac{d^n f(t)}{dt^n} = \lim_{\Delta t \rightarrow 0} \left[\frac{1}{(\Delta t)^n} \sum_{j=0}^n (-1)^j \binom{n}{j} f(t - j\Delta t) \right] \quad (4)$$

where the binomial coefficient

$$\binom{n}{j} = \begin{cases} \frac{n!}{j!(n-j)!} & \text{for } 0 \leq j \leq n \\ 0 & \text{for } 0 \leq n < j \end{cases} \quad (5)$$

is used. If we replace the time step Δt by the fraction $\frac{t}{N}$, $N = 1, 2, 3, \dots$, equation (4) can be written as

$$\frac{d^n f(t)}{dt^n} = \lim_{N \rightarrow \infty} \left[\left(\frac{t}{N} \right)^{-n} \sum_{j=0}^{N-1} (-1)^j \binom{n}{j} f(t - j\frac{t}{N}) \right] \quad (6)$$

noting that

$$\binom{n}{j} = 0 \quad \text{for } j > n \quad (7)$$

The upper limit of the sum $N - 1$ seems to be somewhat arbitrary. However, it derives from defining the lower limit of an integral, when (6) is used to define integrals as a limit of a Riemann sum, see Oldham & Spanier (1974) or Podlubny (1999).

In order to deduce a formulation that is valid for any real order derivative, we use the extended definition of the binomial coefficient

$$\binom{a}{j} = \begin{cases} \frac{a(a-1)(a-2)\dots(a-j+1)}{j} & \text{for } j > 0 \\ 1 & \text{for } j = 0 \end{cases} \quad (8)$$

wherein a is real and j is a natural number. For $j > 0$ the expression $(-1)^j \binom{n}{j}$ can then be written as

$$\begin{aligned} (-1)^j \binom{n}{j} &= \overbrace{\frac{n(n-1)(n-2)\dots(n-j+2)(n-j+1)}{j!}}^{j \text{ factors}} \\ &= \frac{(j-n-1)(j-n-2)\dots(-n+1)(-n)}{j!} \\ &= \binom{j-n-1}{j} \equiv \frac{\Gamma(j-n)}{\Gamma(-n)\Gamma(j+1)} \quad (9) \end{aligned}$$

such that Γ is the gamma function. For $j = 0$ equation (9) of course holds as well. Inserting (9) into (6),

we obtain

$$\frac{d^n f(t)}{dt^n} = \lim_{N \rightarrow \infty} \left[\left(\frac{t}{N} \right)^{-n} \sum_{j=0}^{N-1} \frac{\Gamma(j-n)}{\Gamma(-n)\Gamma(j+1)} f(t - j\frac{t}{N}) \right] \quad (10)$$

which is valid for any real-order derivative ($n > 0$). If we now reinterpret n to be any real number ν , the Grünwald definition (Grünwald 1867) of fractional derivatives (and integrals) is derived

$$\frac{d^\nu f(t)}{dt^\nu} = \lim_{N \rightarrow \infty} \left[\left(\frac{t}{N} \right)^{-\nu} \sum_{j=0}^{N-1} A_{j+1} f(t - j\frac{t}{N}) \right], \quad (11)$$

wherein

$$A_{j+1} \equiv \frac{\Gamma(j-\nu)}{\Gamma(-\nu)\Gamma(j+1)} \quad (12)$$

are the so-called Grünwald coefficients A_{j+1} .

As indicated above, Equation (10) is also valid for integer-order integrals, as can be seen directly from the Riemann definition of an integral, where the lower limit is taken to be zero. In this case, n ranges from -1 to $-\infty$ and Equation (11) can be interpreted as a definition of either fractional integrals and derivatives, where ν ranges from $-\infty$ to ∞ .

Note in this context, that all Grünwald coefficients A_{j+1} are different from zero as long as the order of derivative ν is not a positive integer. If, e.g. $\nu = -1$, then $A_{j+1} = 1$ for all j , according to the Riemann sum.

For ν being a natural number n , only the first $n+1$ Grünwald coefficients A_{j+1} are non-zero, indicating a local operator. On the other hand, as for any positive non-integer number all coefficients A_{j+1} are non-zero, fractional derivatives are non-local operators, except for integer-order derivatives. Analogous to the fractional integral, the lower limit (also called ‘terminal’) of the fractional derivative in (11) is zero. This is indicated by the function values taken into account in the sum in Equation (11), i.e. the first addend ($j = 0$) is $A_1 f(t)$ and the last ($j = N-1$) is $A_N f(t - \frac{N-1}{N}t) = A_N f(\frac{t}{N})$. Thus, the interval $(0, t]$ is divided into N sections of equal size for the calculation of the fractional derivative or integral.

In this paper the lower terminal is assumed to be zero. This may be indicated using the differential operator representation

$$\begin{aligned} {}_0D_t^\nu &= \frac{d^\nu f(t)}{dt^\nu} \\ &= \lim_{N \rightarrow \infty} \left[\left(\frac{t}{N} \right)^{-\nu} \sum_{j=0}^{N-1} A_{j+1} f(t - j\frac{t}{N}) \right] \end{aligned} \quad (13)$$

such that the lower indices 0 and t indicate the lower and upper terminal of the fractional differential operator, respectively.

3 NUMERICAL EVALUATION OF FRACTIONAL DERIVATIVES

Analogous to the numerical evaluation of integrals, fractional derivatives can be calculated by approximating the infinite sum in Equation (11) by a finite sum, such that $N < \infty$,

$$\frac{d^\nu f(t)}{dt^\nu} \approx \left[\left(\frac{t}{N} \right)^{-\nu} \sum_{j=0}^{N-1} A_{j+1} f(t - j\frac{t}{N}) \right] \quad (14)$$

The relative roundoff error R using Equation (14) can be approximated by comparing the results of successive approximations, calculated with N and $N + \Delta N$ addends in the sum

$$R(N, \Delta N) = \frac{[{}_0D_t^\nu f(t)]_{(N)} - [{}_0D_t^\nu f(t)]_{(N+\Delta N)}}{[{}_0D_t^\nu f(t)]_{(N+\Delta N)}}, \quad (15)$$

such that $[{}_0D_t^\nu f(t)]_{(N)}$ is calculated with N addends in the sum while $[{}_0D_t^\nu f(t)]_{(N+\Delta N)}$ uses $N + \Delta N$ addends.

Further reduction of the calculation effort is motivated by the property of the ‘fading memory’. Using

$$\Gamma(x) = (x-1)\Gamma(x-1) \quad (16)$$

we obtain the recursive relationship

$$\begin{aligned} A_{j+1} &= \frac{\Gamma(j-\nu)}{\Gamma(-\nu)\Gamma(j+1)} = \frac{j-1-\nu}{j} \frac{\Gamma(j-1-\nu)}{\Gamma(-\nu)\Gamma(j)} \\ &= \frac{j-1-\nu}{j} A_j \end{aligned} \quad (17)$$

If we restrict ourselves to fractional derivatives, i.e. $\nu > 0$, one can see that

$$|A_{j+1}| = \left| \frac{j-1-\nu}{j} \right| |A_j| < |A_j| \quad \text{for } j > \nu. \quad (18)$$

This means that the series given by $|A_{j+1}|$ is strictly decreasing from the moment where j becomes larger than the order of derivative ν . The limit $j \rightarrow \infty$ of the series follows from the estimation

$$\begin{aligned} \lim_{j \rightarrow \infty} |A_{j+1}| &= \left| \frac{1}{\Gamma(-\nu)} \right| \lim_{j \rightarrow \infty} \left| \frac{\Gamma(j-\nu)}{\Gamma(j+1)} \right| \\ &< \left| \frac{1}{\Gamma(-\nu)} \right| \lim_{j \rightarrow \infty} \left| \frac{\Gamma(j)}{\Gamma(j+1)} \right| \end{aligned}$$

for $j > \nu + 2$, as the gamma function $\Gamma(x)$ is strictly non-decreasing for $x \leq 2$. Because of $j \in \mathbb{N}$, we can write $\Gamma(j+1) = j!$ and thus

$$\begin{aligned} \lim_{j \rightarrow \infty} |A_{j+1}| &< \left| \frac{1}{\Gamma(-\nu)} \right| \lim_{j \rightarrow \infty} \left| \frac{(j-1)!}{j!} \right| = \\ &= \left| \frac{1}{\Gamma(-\nu)} \right| \lim_{j \rightarrow \infty} \left(\frac{1}{j} \right) = 0. \end{aligned} \quad (19)$$

As with growing j the Grünwald coefficients weight function values that are situated further in the past, events are faded out as time goes by. This property is called the ‘fading memory’ and motivates the truncation of (14)

$$\frac{d^\nu f(t)}{dt^\nu} \approx \left(\frac{t}{N}\right)^{-\nu} \sum_{j=0}^{N_\ell} A_{j+1} f\left(t - j\frac{t}{N}\right) \quad , \quad (20)$$

where $N_\ell < N - 1$. The error E of approximation (20) compared to (14) is given by

$$E(N, N_\ell) = \left(\frac{t}{N}\right)^{-\nu} \sum_{j=N_\ell+1}^{N-1} A_{j+1} f\left(t - j\frac{t}{N}\right) \quad (21)$$

and can be estimated by

$$|E(N, N_\ell)| \leq \left|\left(\frac{t}{N}\right)^{-\nu}\right| \sum_{j=N_\ell+1}^{N-1} |A_{j+1} f\left(t - j\frac{t}{N}\right)| \quad . \quad (22)$$

Since t and N are positive numbers

$$|E(N, N_\ell)| \leq \left(\frac{t}{N}\right)^{-\nu} (N - N_\ell - 1) \max |A_{j+1} f\left(t - j\frac{t}{N}\right)| \quad ,$$

$$j \in [N_\ell + 1, N - 1] \quad . \quad (23)$$

4 FRACTIONAL VISCOELASTIC CONSTITUTIVE EQUATIONS

Usually, rheological models of linear viscoelasticity consist of springs and dashpots. The constitutive equations of these elements may be generalized (see Figure 1) using fractional derivatives. The resulting fractional constitutive equation

$$\sigma = p \frac{d^\nu}{dt^\nu} \varepsilon \quad (24)$$

includes p as a proportionality factor and ν as the order of derivative which is commonly taken to range between 0 and 1. If ν is 0, Equation (24) describes the behavior of a spring where p specifies the springs’ stiffness. For $\nu = 1$, (24) defines the constitutive equation of a dashpot, in which p defines the viscosity. Thus, the fractional constitutive equation (24) ‘interpolates’ between the material behavior of a spring and that of a dashpot. The rheological element which refers to Equation (24) was therefore introduced by Koeller (1984) as a ‘spring-pot’.

By replacing the dashpots in rheological models by spring-pots, fractional rheological models are derived. Application to the classical 3-parameter model (see Figure 2) results in

$$\sigma + \frac{p}{E_1 + E_2} \frac{d^\nu}{dt^\nu} \sigma = \frac{E_1 E_2}{E_1 + E_2} \varepsilon + \frac{p E_2}{E_1 + E_2} \frac{d^\nu}{dt^\nu} \varepsilon \quad (25)$$

which will be called the constitutive equation of the fractional 3-parameter model in what follows. Since the spring-pot contains 2 parameters p and ν , the fractional 3-parameter model in fact is a 4-parameter model. By introducing the constants

$$a = \frac{p}{E_1 + E_2} \quad , \quad b = \frac{p E_2}{E_1 + E_2} \quad \text{and}$$

$$c = \frac{E_1 E_2}{E_1 + E_2}$$

equation (25) simplifies to

$$\sigma + a \frac{d^\nu}{dt^\nu} \sigma = c \varepsilon + b \frac{d^\nu}{dt^\nu} \varepsilon \quad . \quad (26)$$

Improved adaptivity to measured material behavior may be realized by fractional Kelvin-chains or different fractional Maxwell elements in parallel. However, as can be seen from the literature, the fractional 3-parameter model already leads to good curve-fitting properties.

An extension of Equation (26) to three dimensions, differentiating between the hydrostatic parts (index h) and the deviatoric parts (index d) of the stresses and strains leads to

$$\underline{\sigma}_h + \underline{A}_h \frac{d^{\nu_h}}{dt^{\nu_h}} \underline{\sigma}_h = \underline{C}_h \varepsilon_h + \underline{B}_h \frac{d^{\nu_h}}{dt^{\nu_h}} \varepsilon_h \quad (27)$$

$$\underline{\sigma}_d + \underline{A}_d \frac{d^{\nu_d}}{dt^{\nu_d}} \underline{\sigma}_d = \underline{C}_d \varepsilon_d + \underline{B}_d \frac{d^{\nu_d}}{dt^{\nu_d}} \varepsilon_d \quad , \quad (28)$$

where underlined lower case letters denote vectors and underlined capital letters denote matrices. The matrices \underline{A} , \underline{B} and \underline{C} depend on the material behavior. If we restrict ourselves to isotropic materials, the

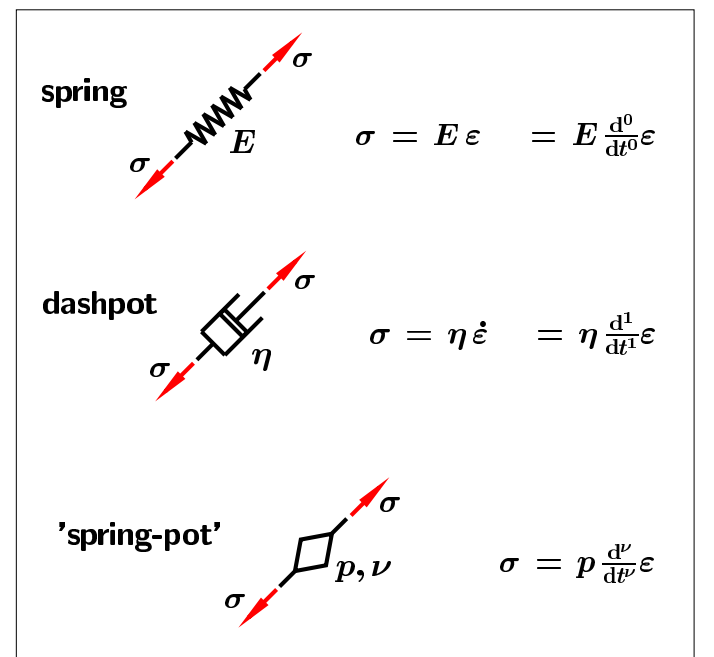


Figure 1. Rheological elements of viscoelasticity

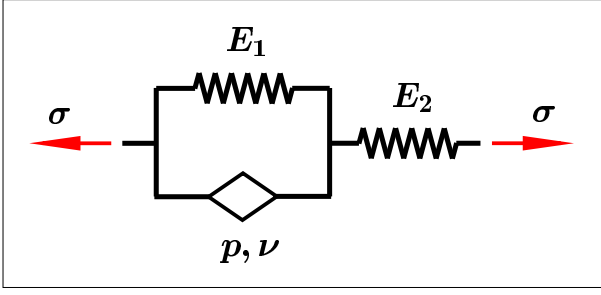


Figure 2. Fractional 3-parameter model

hydrostatic and the deviatoric parts of the stresses and strains are calculated from the stress vector

$$\underline{\sigma} = [\sigma_{xx} \ \sigma_{yy} \ \sigma_{zz} \ \sigma_{xy} \ \sigma_{yz} \ \sigma_{zx}]^T \quad (29)$$

and the strain vector

$$\underline{\varepsilon} = [\varepsilon_{xx} \ \varepsilon_{yy} \ \varepsilon_{zz} \ \varepsilon_{xy} \ \varepsilon_{yz} \ \varepsilon_{zx}]^T \quad (30)$$

using the relationships

$$\underline{\sigma}_h = \underline{T}_h \underline{\sigma} \quad , \quad \underline{\sigma}_d = \underline{T}_d \underline{\sigma} \quad ,$$

$$\underline{\varepsilon}_h = \underline{T}_h \underline{\varepsilon} \quad , \quad \underline{\varepsilon}_d = \underline{T}_d \underline{\varepsilon} \quad ,$$

where

$$\underline{T}_h = \begin{bmatrix} \frac{1}{3} & \frac{1}{3} & \frac{1}{3} & 0 & 0 & 0 \\ \frac{1}{3} & \frac{1}{3} & \frac{1}{3} & 0 & 0 & 0 \\ \frac{1}{3} & \frac{1}{3} & \frac{1}{3} & 0 & 0 & 0 \\ 0 & 0 & 0 & 0 & 0 & 0 \\ 0 & 0 & 0 & 0 & 0 & 0 \\ 0 & 0 & 0 & 0 & 0 & 0 \end{bmatrix} \quad ,$$

$$\underline{T}_d = \begin{bmatrix} \frac{2}{3} & -\frac{1}{3} & -\frac{1}{3} & 0 & 0 & 0 \\ -\frac{1}{3} & \frac{2}{3} & -\frac{1}{3} & 0 & 0 & 0 \\ -\frac{1}{3} & -\frac{1}{3} & \frac{2}{3} & 0 & 0 & 0 \\ 0 & 0 & 0 & 1 & 0 & 0 \\ 0 & 0 & 0 & 0 & 1 & 0 \\ 0 & 0 & 0 & 0 & 0 & 1 \end{bmatrix} \quad .$$

In addition, for isotropic materials the matrices \underline{A} , \underline{B} and \underline{C} become multiples of the identity matrix \underline{I} and can be written as

$$\underline{A}_h = a_h \underline{I} \quad , \quad \underline{A}_d = a_d \underline{I}$$

$$\underline{B}_h = b_h \underline{I} \quad , \quad \underline{B}_d = b_d \underline{I}$$

$$\underline{C}_h = c_h \underline{I} \quad , \quad \underline{C}_d = c_d \underline{I} \quad .$$

Equations (27) and (28) are linked by the stress state $\underline{\sigma} = \underline{\sigma}_h + \underline{\sigma}_d$ and the strain state $\underline{\varepsilon} = \underline{\varepsilon}_h + \underline{\varepsilon}_d$. Adding (27) and (28) leads to

$$\underline{\sigma} + \left(a_h \underline{T}_h \frac{d^{v_h}}{dt^{v_h}} + a_d \underline{T}_d \frac{d^{v_d}}{dt^{v_d}} \right) \underline{\sigma} = \underline{C} \underline{\varepsilon} + \left(b_h \underline{T}_h \frac{d^{v_h}}{dt^{v_h}} + b_d \underline{T}_d \frac{d^{v_d}}{dt^{v_d}} \right) \underline{\varepsilon} \quad , \quad (31)$$

wherein

$$\underline{C} = c_h \underline{T}_h + c_d \underline{T}_d \quad (32)$$

describes the instantaneous relationship between the stresses and strains. If the material is purely elastic, i.e. $a_h = a_d = b_h = b_d = 0$, comparison with Hooke's law results in

$$c_h = 3K \quad , \quad c_d = 2G \quad (33)$$

with K as the bulk modulus and G as the shear modulus.

As mentioned earlier, the Kelvin-Voigt model is enclosed in the 3-parameter model. In contrast to the latter, the Kelvin-Voigt model only contains derivatives of the strains. Thus, the generalized Kelvin-Voigt model using fractional derivatives is obtained by setting the respective factors to zero, i.e. $a_h = a_d = 0$.

5 FINITE-ELEMENT FORMULATION

In the foregoing chapter, viscoelastic constitutive equations were deduced that may be integrated into FE formulations. The resulting equation of motion can be solved using direct integration methods. The displacement type formulation is based on

$$\underline{u} = \underline{H} \hat{\underline{u}} \quad , \quad (34)$$

where \underline{u} denotes the displacement field of an element, $\hat{\underline{u}}$ is the vector of the nodal displacements and \underline{H} specifies the shape functions. The strain field $\underline{\varepsilon}$ and the nodal displacements are linked by

$$\underline{\varepsilon} = \underline{B} \hat{\underline{u}} \quad , \quad (35)$$

such that \underline{B} defines the appropriate spatial derivatives of \underline{H} . The principle of virtual work yields the equation of motion

$$\int_V \underline{B}^T \underline{\sigma} dV + \underline{M} \ddot{\underline{u}} = \underline{r} \quad (36)$$

where V is the region in which the element is defined and \underline{r} defines the external and body forces. The consistent mass matrix \underline{M} is given by

$$\underline{M} = \int_V \underline{H}^T \rho \underline{H} dV \quad , \quad (37)$$

ρ denoting the mass density of the material. To simplify matters, in the following the accent $\hat{\cdot}$ is skipped. At time t , indexed on the upper left of the variable, the equation of motion results in

$$\int_V \underline{B}^T {}^t \underline{\sigma} dV + \underline{M} {}^t \ddot{\underline{u}} = {}^t \underline{r} \quad . \quad (38)$$

The stress vector ${}^t\boldsymbol{\underline{\sigma}}$ is derived from the viscoelastic constitutive equation (31), using the time discrete Grünwaldian formulation of fractional derivatives (20). This yields

$$\begin{aligned} {}^t\boldsymbol{\underline{\sigma}} + a_h \left(\frac{t}{N}\right)^{-v_h} \boldsymbol{\underline{T}}_h \sum_{j=0}^{N_\ell} A_{j+1}^{(v_h)} t^{-j\frac{t}{N}} \boldsymbol{\underline{\sigma}} + \\ + a_d \left(\frac{t}{N}\right)^{-v_d} \boldsymbol{\underline{T}}_d \sum_{j=0}^{N_\ell} A_{j+1}^{(v_d)} t^{-j\frac{t}{N}} \boldsymbol{\underline{\sigma}} = \\ \boldsymbol{\underline{C}}^t \boldsymbol{\underline{\varepsilon}} + b_h \left(\frac{t}{N}\right)^{-v_h} \boldsymbol{\underline{T}}_h \sum_{j=0}^{N_\ell} A_{j+1}^{(v_h)} t^{-j\frac{t}{N}} \boldsymbol{\underline{\varepsilon}} + \\ + b_d \left(\frac{t}{N}\right)^{-v_d} \boldsymbol{\underline{T}}_d \sum_{j=0}^{N_\ell} A_{j+1}^{(v_d)} t^{-j\frac{t}{N}} \boldsymbol{\underline{\varepsilon}} \quad (39) \end{aligned}$$

which can be solved explicitly for ${}^t\boldsymbol{\underline{\sigma}}$. Using Equation (35) and the identity $A_1 \stackrel{!}{=} 1$ one obtains

$$\begin{aligned} {}^t\boldsymbol{\underline{\sigma}} = & \left[\boldsymbol{\underline{I}} + a_h \left(\frac{t}{N}\right)^{-v_h} \boldsymbol{\underline{T}}_h + a_d \left(\frac{t}{N}\right)^{-v_d} \boldsymbol{\underline{T}}_d \right]^{-1} \cdot \\ & \cdot \left[\left(\boldsymbol{\underline{C}} + b_h \left(\frac{t}{N}\right)^{-v_h} \boldsymbol{\underline{T}}_h + b_d \left(\frac{t}{N}\right)^{-v_d} \boldsymbol{\underline{T}}_d \right) \boldsymbol{\underline{B}}^t \boldsymbol{\underline{u}} \right. \\ & + b_h \left(\frac{t}{N}\right)^{-v_h} \boldsymbol{\underline{T}}_h \boldsymbol{\underline{B}} \sum_{j=1}^{N_\ell} A_{j+1}^{(v_h)} t^{-j\frac{t}{N}} \boldsymbol{\underline{u}} \\ & + b_d \left(\frac{t}{N}\right)^{-v_d} \boldsymbol{\underline{T}}_d \boldsymbol{\underline{B}} \sum_{j=1}^{N_\ell} A_{j+1}^{(v_d)} t^{-j\frac{t}{N}} \boldsymbol{\underline{u}} \\ & - a_h \left(\frac{t}{N}\right)^{-v_h} \boldsymbol{\underline{T}}_h \sum_{j=1}^{N_\ell} A_{j+1}^{(v_h)} t^{-j\frac{t}{N}} \boldsymbol{\underline{\sigma}} \\ & \left. - a_d \left(\frac{t}{N}\right)^{-v_d} \boldsymbol{\underline{T}}_d \sum_{j=1}^{N_\ell} A_{j+1}^{(v_d)} t^{-j\frac{t}{N}} \boldsymbol{\underline{\sigma}} \right] \quad (40) \end{aligned}$$

equations (40) and (38) yield

$$\boldsymbol{\underline{M}}^t \ddot{\boldsymbol{\underline{u}}} + \boldsymbol{\underline{K}}^* \boldsymbol{\underline{u}} = \boldsymbol{\underline{r}}^* \quad (41)$$

wherein

$$\boldsymbol{\underline{K}}^* = \int_V \boldsymbol{\underline{B}}^T \boldsymbol{\underline{F}}^{-1} \boldsymbol{\underline{C}}^* \boldsymbol{\underline{B}} \, dV \quad (42)$$

is the modified stiffness matrix that includes the abbreviations

$$\boldsymbol{\underline{F}} = \left(\boldsymbol{\underline{I}} + a_h \left(\frac{t}{N}\right)^{-v_h} \boldsymbol{\underline{T}}_h + a_d \left(\frac{t}{N}\right)^{-v_d} \boldsymbol{\underline{T}}_d \right), \quad (43)$$

$$\boldsymbol{\underline{C}}^* = \left(\boldsymbol{\underline{C}} + b_h \left(\frac{t}{N}\right)^{-v_h} \boldsymbol{\underline{T}}_h + b_d \left(\frac{t}{N}\right)^{-v_d} \boldsymbol{\underline{T}}_d \right). \quad (44)$$

The modified force vector $\boldsymbol{\underline{r}}^*$ results in

$$\begin{aligned} \boldsymbol{\underline{r}}^* = & \boldsymbol{\underline{r}} - \boldsymbol{\underline{\Phi}}_h b_h \left(\frac{t}{N}\right)^{-v_h} \sum_{j=1}^{N_\ell} A_{j+1}^{(v_h)} t^{-j\frac{t}{N}} \boldsymbol{\underline{u}} - \\ & - \boldsymbol{\underline{\Phi}}_d \sum b_d \left(\frac{t}{N}\right)^{-v_d} \sum_{j=1}^{N_\ell} A_{j+1}^{(v_d)} t^{-j\frac{t}{N}} \boldsymbol{\underline{u}} + \\ & + \int_V \boldsymbol{\underline{B}}^T \boldsymbol{\underline{F}}^{-1} \left(a_h \left(\frac{t}{N}\right)^{-v_h} \boldsymbol{\underline{T}}_h \sum_{j=1}^{N_\ell} A_{j+1}^{(v_h)} t^{-j\frac{t}{N}} \boldsymbol{\underline{\sigma}} + \right. \\ & \left. + a_d \left(\frac{t}{N}\right)^{-v_d} \boldsymbol{\underline{T}}_d \sum_{j=1}^{N_\ell} A_{j+1}^{(v_d)} t^{-j\frac{t}{N}} \boldsymbol{\underline{\sigma}} \right) \, dV. \quad (45) \end{aligned}$$

such that

$$\boldsymbol{\underline{\Phi}}_h = \int_V \boldsymbol{\underline{B}}^T \boldsymbol{\underline{F}}^{-1} \boldsymbol{\underline{T}}_h \boldsymbol{\underline{B}} \, dV \quad (46)$$

and

$$\boldsymbol{\underline{\Phi}}_d = \int_V \boldsymbol{\underline{B}}^T \boldsymbol{\underline{F}}^{-1} \boldsymbol{\underline{T}}_d \boldsymbol{\underline{B}} \, dV \quad (47)$$

Note, in contrast to the integral over the stresses that has to be calculated explicitly at each time, the integral over the strains can be simplified by decomposing the strains $\boldsymbol{\underline{\varepsilon}}(\boldsymbol{x}, t) = \boldsymbol{\underline{B}}(\boldsymbol{x}) \boldsymbol{\underline{u}}(t)$ and carrying out the integral once for each element, obtaining the matrices $\boldsymbol{\underline{\Phi}}_h$ and $\boldsymbol{\underline{\Phi}}_d$.

The matrix $\boldsymbol{\underline{K}}^*$ can be considered as a modified (initial) stiffness matrix. The additional terms on the right-hand side of Equation (45) depend on the hydrostatic and the deviatoric strain and stress history. If they are interpreted as additional external forces, Equation (41) is a purely elastic equation of motion. On the other hand, this means that these additional external forces describe the time-dependent material behavior.

As mentioned in chapter 4, the generalized Kelvin-Voigt model using fractional derivatives is obtained by setting $a_h = a_d = 0$. Hence $\boldsymbol{\underline{F}} = \boldsymbol{\underline{I}}$ and the integral in Equation (45) vanishes. From this it follows that the numerical effort for solving the equation of motion (41) decreases substantially using the fractional Kelvin-Voigt model instead of the fractional 3-parameter model. In addition, the memory requirements are decreasing, since only the nodal displacements have to be stored at each discrete point of time while with the fractional 3-parameter model the stress history has to be stored at each integration point as well.

Either from Equation (41) and the subsequent definitions or directly from Equations (38) and (31) it follows that the equation of motion for the Kelvin-Voigt

model can be written as

$$\begin{aligned} \underline{M}^t \ddot{\underline{u}} + \underline{\Phi}_h b_h \frac{d^{v_h}}{dt^{v_h}} \dot{\underline{u}} + \\ + \underline{\Phi}_d b_d \frac{d^{v_d}}{dt^{v_d}} \dot{\underline{u}} + \underline{K}^t \underline{u} = \underline{r}^t \quad , \quad (48) \end{aligned}$$

where

$$\underline{K} = \int_V \underline{B}^T \underline{C} \underline{B} \, dV \quad (49)$$

defines the stiffness matrix. Equation (48) can be considered as a generalization of the equation of motion using velocity-proportional damping, such as the Rayleigh damping, which is often used in standard FE-codes.

6 IMPLEMENTATION

The Implementation of Equation (41) into an FE code using direct integration procedures is similar to the implementation of purely elastic equation of motions, except for the calculation of the modified stiffness matrix and the modified force vector. While the modified stiffness matrix is calculated once for each element and stays constant with time, the modified force vector depends on the strain and stress history up to the time t and thus does not affect the resolution for the new displacement at time $t + \Delta t$. Consequently, the modified force vector may be calculated at the beginning of each time step.

As the equation of motion (41) may also be established at time $t + \Delta t$, there is no restriction in the applied integration scheme, i.e. equation (41) may be used in conjunction with either explicit and implicit integration schemes.

As a consequence of the Grünwaldian formulation of fractional derivatives, the strain and stress history is needed at equidistant discrete times. The time step, separating two successive function values, is defined as $\frac{t}{N}$ and may be different from the time step Δt used for time integration. However, it is expedient taking the time step of the fractional derivatives to be equal to or a whole-numbered multiple of the time step Δt

$$\frac{t}{N} = n\Delta t \quad , \quad n \in \mathbb{N} \quad , \quad (50)$$

particularly if Δt is constant during the calculation. In case of a changing time step Δt , the strain and stress history has to be calculated at other discrete times. This might be done using linear or quadratic approximation.

At the end of each time step the actual displacements and thus the strains are known. The actual stresses ${}^{t+\Delta t}\underline{\sigma}$ that are needed in the next increment to specify the new modified force vector ${}^t\underline{r}^*$ have to be calculated from the constitutive equation (40) as a

function of the actual strains ${}^{t+\Delta t}\underline{\epsilon}$ and the strain and stress history. Letting

$$\frac{t}{N} = \Delta t \quad (51)$$

this reads

$$\begin{aligned} {}^{t+\Delta t}\underline{\sigma} = f({}^{t+\Delta t}\underline{\epsilon}, {}^t\underline{\epsilon}, {}^{t-\Delta t}\underline{\epsilon}, {}^{t-2\Delta t}\underline{\epsilon}, \dots \\ \dots, {}^t\underline{\sigma}, {}^{t-\Delta t}\underline{\sigma}, {}^{t-2\Delta t}\underline{\sigma}, \dots) \quad . \quad (52) \end{aligned}$$

6.1 Newmark algorithm

Exemplarily the implementation into the implicit Newmark algorithm is demonstrated. Starting point is the definition of the new velocity vector ${}^{t+\Delta t}\underline{\dot{u}}$ and displacement vector ${}^{t+\Delta t}\underline{u}$

$${}^{t+\Delta t}\underline{\dot{u}} = {}^t\underline{\dot{u}} + (1 - \delta)\Delta t {}^t\underline{\ddot{u}} + \delta\Delta t {}^{t+\Delta t}\underline{\ddot{u}} \quad , \quad (53)$$

$$\begin{aligned} {}^{t+\Delta t}\underline{u} = {}^t\underline{u} + \Delta t {}^t\underline{\dot{u}} + \\ + \left(\frac{1}{2} - \alpha\right) (\Delta t)^2 {}^t\underline{\ddot{u}} + \alpha(\Delta t)^2 {}^{t+\Delta t}\underline{\ddot{u}} \quad (54) \end{aligned}$$

where α and δ denote the Newmark parameters. Solving Equation (54) for the new acceleration vector ${}^{t+\Delta t}\underline{\ddot{u}}$, one obtains

$${}^{t+\Delta t}\underline{\ddot{u}} = a_1({}^{t+\Delta t}\underline{u} - {}^t\underline{u}) - a_2 {}^t\underline{\dot{u}} - a_3 {}^t\underline{\ddot{u}} \quad (55)$$

using the abbreviations

$$\begin{aligned} a_1 &= \frac{1}{\alpha(\Delta t)^2} \quad , \quad a_2 = \frac{1}{\alpha\Delta t} \quad , \\ a_3 &= \frac{1}{2\alpha} - 1 \quad . \end{aligned}$$

If one substitutes (55) into Equation (41) and solves for the new displacement vector ${}^{t+\Delta t}\underline{u}$ yields

$$\begin{aligned} {}^{t+\Delta t}\underline{u} = [a_1\underline{M} + \underline{K}^*]^{-1} \\ \left[{}^{t+\Delta t}\underline{r}^* + \underline{M}(a_1 {}^t\underline{u} + a_2 {}^t\underline{\dot{u}} + a_3 {}^t\underline{\ddot{u}}) \right] \quad (56) \end{aligned}$$

where all variables on the right-hand side are known or can be calculated from Equations (37), (42) and (45).

7 EXAMPLES

7.1 Parameter identification

As mentioned earlier, fractional constitutive equations provide good curve-fitting properties, especially when being applied to a broad range of time or frequencies, typically 5 to 7 decades. This characteristic

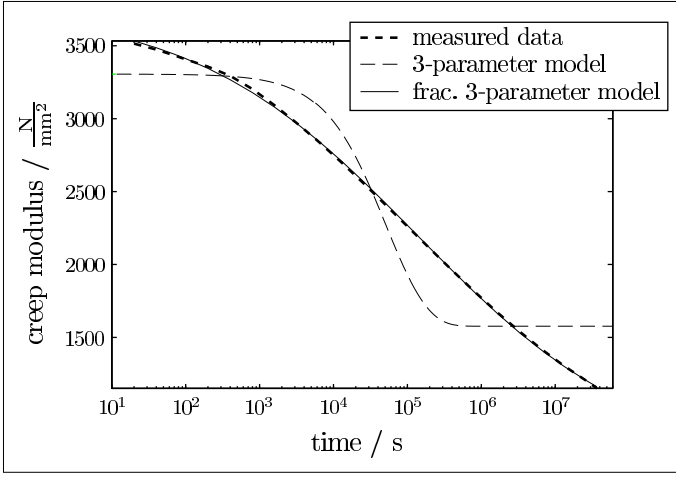


Figure 3. Parameter identification in the time domain

is demonstrated by performing a parameter identification in the time domain. The creep behavior of a polymer at constant temperature is given for the time from 10 s up to 10 000 h, i.e. for a time span of approximately 6.5 decades. The creep curve is displayed in terms of the creep modulus E_c

$$E_c = \frac{\sigma}{\varepsilon(t)} \quad (57)$$

wherein σ is the time independent stress (see Figure 3). The fractional constitutive equation is given by the fractional 3-parameter model (26). Thus, the constitutive equation

$$\sigma + a \frac{d^v \sigma}{dt^v} = c \varepsilon + b \frac{d^v \varepsilon}{dt^v} \quad (58)$$

contains 4 parameters a , b , c and v that are identified by applying the least-square fit method. The results, specified in Table 1, are displayed in Figure 3 and point out the excellent adaptiveness of fractional constitutive equations. For comparison reasons, the result of a parameter identification of an ‘ordinary’ 3-parameter model, which is known to result in exponential functions, is shown as well. Though the fractional 3-parameter model (58) possesses only one additional parameter, its improved adaptive capability to measured data is significant.

Table 1. Identified parameters in the time domain

Parameter	Value	Dimension
c	658.2	$\frac{N}{mm^2}$
v	0.2845	–
a	32.017	s^v
b	120593.0	$\frac{N}{mm^2} s^v$

A parameter identification in the frequency domain is carried out for the complex modulus of the polymer DelrinTM at a temperature of 22°C in a frequency range from approximately 50 to 500 Hz. Assuming sinusoidal stress and strain in time, one may introduce the complex modulus

$$E^* = E' + iE'' \quad (59)$$

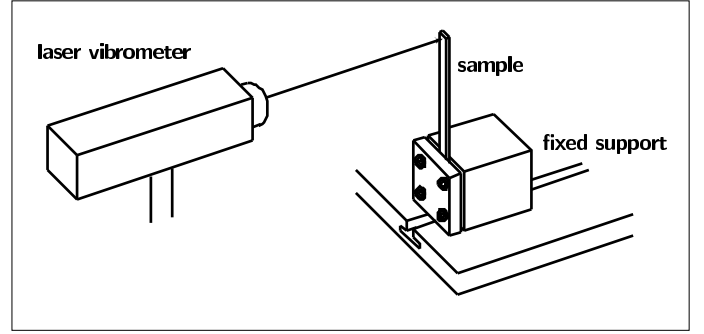


Figure 4. Experimental setup

wherein E' is called the storage modulus, E'' denotes the loss modulus and i is the complex variable. According to the elastic-viscoelastic correspondence principle, the complex modulus depends on the frequency and relates the complex amplitudes of strain σ^* and stress ε^* by

$$\sigma^*(\omega) = E^*(\omega)\varepsilon^*(\omega) \quad (60)$$

Applying the Fourier transformation to the fractional constitutive equation (58) results in

$$E^*(\omega) = \frac{c + b(i\omega)^v}{1 + a(i\omega)^v} \quad (61)$$

Equation (61) is equivalent to the well known Cole-Cole relaxation that was deduced phenomenologically from measurements (Cole & Cole 1941) and which is known to provide good curve-fitting properties. Obviously, this empirical relationship can be derived from the fractional 3-parameter model.

The material properties were detected by performing free-decay tests with 6 cantilevers made of DelrinTM. Each of the cantilevers was fixed at different lengths in order to excite oscillations at different frequencies that were measured by a laser vibrometer, see Figure 4. All tests were repeated 5 times. The storage and the loss modulus were deduced from the frequency and the decaying behavior of the oscillation, respectively. The data points in Figures 5 and 6 were then calculated as the average of the multiple results at each frequency.

In order to minimize initial effects, the first 20 oscillations after the initial deflection of the cantilevers were truncated. Thus, a single frequency signal was obtained.

The material parameters of the complex modulus (61) again were identified in terms of a least-square fit for both, the storage and the loss modulus. The results are listed in Table 2 and displayed in the Figures 5 and 6, where once more the result of an identified ‘ordinary’ 3-parameter model is given.

The difference between a fractional and an integer-order model would be much more impressive, if one would apply the models to a larger frequency range, see e.g. Cupial (1996).

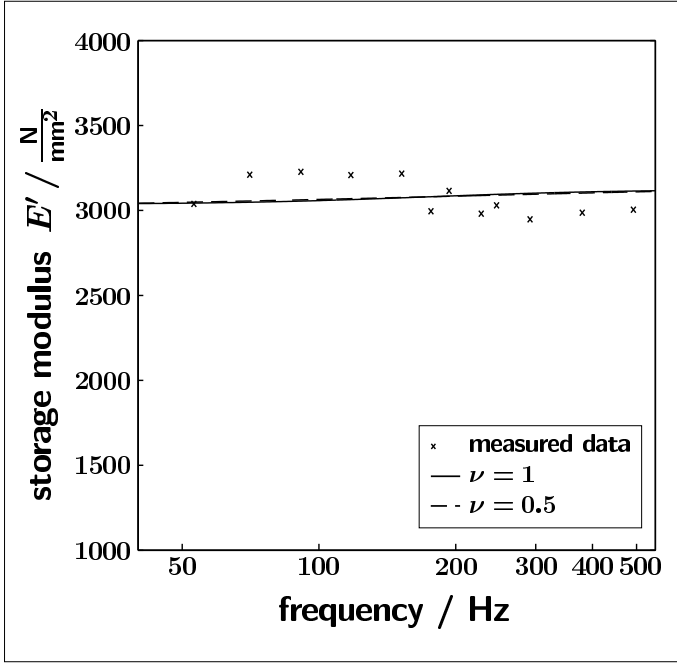


Figure 5. Storage modulus

Table 2. Identified parameters in the frequency domain

Parameter	Value	Dimension
c	2981.6	$\frac{N}{mm^2}$
ν	0.4835	–
a	0.02838	s^ν
b	90.31	$\frac{N}{mm^2} s^\nu$

7.2 Finite-Element calculation

As a benchmark of the three-dimensional implementation described in the foregoing chapters, one of the free-decay tests is calculated using the fractional 3-parameter model in conjunction with the identified

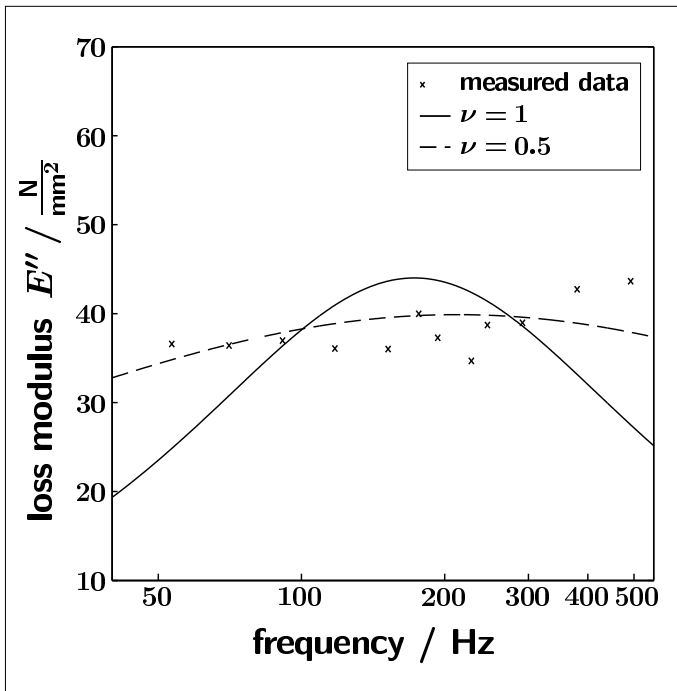


Figure 6. Loss modulus

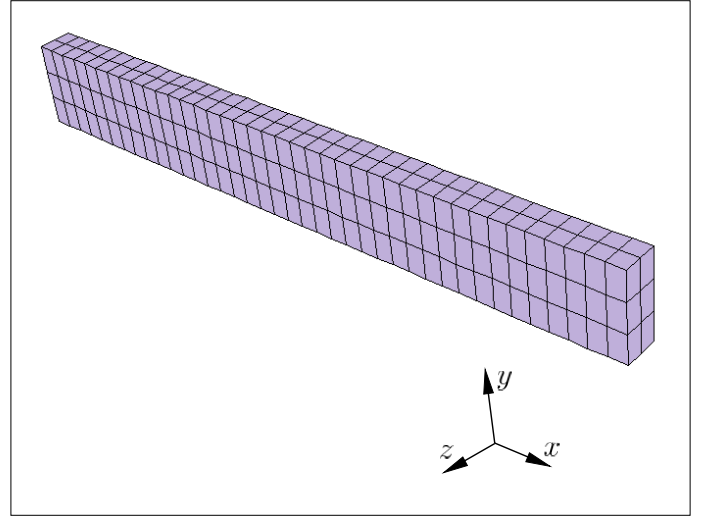


Figure 7. Finite Element model

parameters, see Table 2. Since the three dimensional constitutive equation (31) needs more material constants than given in Table 2, the hydrostatic and deviatoric functions are taken to be identical, i.e.

$$a_h = a_d = a \quad , \quad b_h = b_d = b$$

$$\nu_h = \nu_d = \nu \quad .$$

The discretization is realized using isoparametric 20-noded hexahedron elements, that approximate the displacements with quadratic functions. The model, shown in Figure 7, is fixed at the left side, employing displacement type boundary conditions. At the right side a point load in z -direction is applied to model the instantaneous deflection. Then, the system is left to its own resource and the time integration is performed using the Newmark method for time integration. In order to prevent numerical damping, the Newmark parameters are

$$\delta = \frac{1}{2} \quad , \quad \alpha = \frac{1}{4} \quad . \quad (62)$$

The measured and the calculated tip deflection of the cantilever are displayed in Figure 8. In addition, the calculated free-decay oscillation is used to detect the complex modulus that is compared to the measured complex modulus in Table 3. The results of the FE calculation can be found to be in good agreement with the experiment. Since a finite element approximation always leads to a stiffer systems behavior, the calculation results in a somewhat higher frequency.

Table 3. Complex modulus identified from the measurement and the calculation

	f / Hz	$E' / \frac{N}{mm^2}$	$E'' / \frac{N}{mm^2}$
measurement	175.9	2977	36.1
calculation	177.6	3037	33.4
rel. error / %	1.0	2.0	7.4

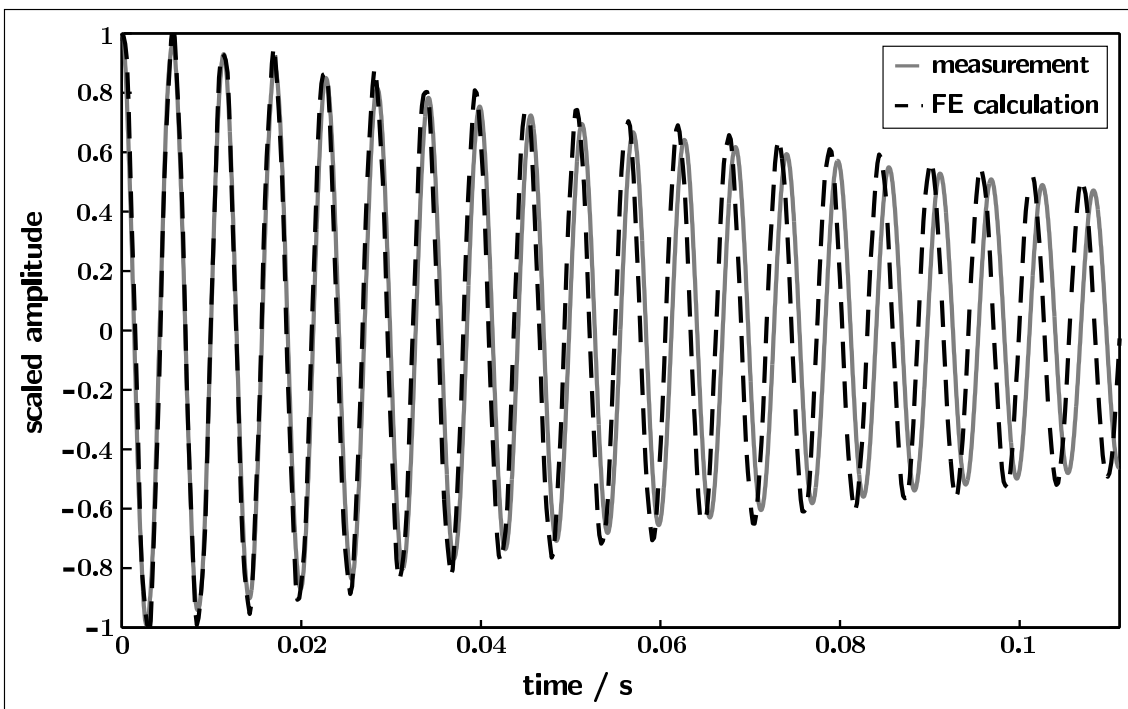


Figure 8. Comparison between measured and calculated tip deflection

Due to the numerical effort and the amount of data, only approximately 20 oscillations were calculated within 600 time increments. As can be seen from Figure 8, initial effects are still present in the calculation, resulting in a frequency spectrum and thus in a perturbation of the decaying behavior. Since for the detection of the loss modulus an exponential function is approximated to the maxima of the signal, its calculated value differs somewhat from the measured behavior.

8 CONCLUSIONS

Fractional time derivatives were used to deduce a new generalized rheological element, which 'interpolates' between a spring and a dashpot and thus was called a 'spring-pot' (Koeller 1984). By replacing the dampers in traditional viscoelastic models by spring-pots, fractional rheological models are obtained. The constitutive equations of these models are represented by fractional differential equations. These so-called fractional constitutive equations were expanded for three-dimensional problems, differentiating between the hydrostatic and the deviatoric parts. We have shown that fractional derivatives result in non-local operators that provide the property of the 'fading memory' as it is known from viscoelastic media. A time discrete approximation for fractional time derivatives was deduced using the Grünwaldian formulation. Thus, we obtained a time discrete constitutive equation which can be implemented into FE formulations. As we demonstrated, the arising equation of motion can be solved by direct time integration, using either implicit or explicit time integration schemes. The implementation for the implicit Newmark algorithm was exemplarily specified.

Two parameter identifications in the time domain

as well as in the frequency domain demonstrate the improved curve-fitting properties of fractional constitutive equations compared to integer-order constitutive equations. Finally, a three dimensional FE time-stepping analysis has been carried out in order to verify the implementation of the fractional constitutive equations. The results were found to be in good agreement with experimental data. However, it has to be mentioned that due to the non-locality of fractional derivatives, the storage requirements and the numerical costs increase significantly.

9 ACKNOWLEDGEMENT

The authors would like to express their gratitude to the company Du Pont and Mr. Class i.e. for providing different material samples that were used in our experiments. The authors would also like to thank the DFG (Deutsche Forschungsgemeinschaft) for their support of this investigation in the framework of the SFB 543 'Ultraschallbeeinflusstes Umformen metallischer Werkstoffe'.

REFERENCES

- Abel, N., 1881. Solution de quelques problèmes à l'aide d'intégrales définites. In Christiania Grondahl (ed), *Oeuvres Complète de Niels Henrik Abel*, Norway.
- Bagley, R. L. & Torvik, P. J., 1983. A theoretical basis for the application of fractional calculus to viscoelasticity. *Journal of Rheology* 27(3): 201–210.
- Bagley, R. L. & Torvik, P. J., 1984. On the appearance of the fractional derivative in the behavior of real materials. *Journal of Applied Mechanics* 51: 294–298.
- Bagley, R. L. & Torvik, P. J., 1986. On the fractional calculus model of viscoelastic behaviour. *Journal of Rheology*

- 30(1): 133–155.
- Caputo, M., 1974. Vibrations on an infinite viscoelastic layer with a dissipative memory. *J. Acoustical Society of America* 56(3): 897–904.
- Caputo, M. & Mainardi, F., 1971a. A new dissipation model based on memory mechanism. *Pure and Applied Geophysics* 91: 134–147.
- Caputo, M. & Mainardi, F., 1971b. Linear models of dissipation in anelastic solids. *Rivista del Nuovo Cimento* 1(2): 161–198.
- Cole, K.S. & Cole, R.H., 1941. Dispersion and absorption in dielectrics. *Journal of Chemical Physics* 9: 341–351.
- Cupial, P., 1996. *Dynamics of Continua*. Some approaches to the analyses of nonproportionally damped viscoelastic structures. Bad Honnef: 93–102.
- Ferry, J.D. & Landel, R.F. & Williams, M.L., 1955. Extensions to the Rouse Theory of viscoelastic properties to undiluted linear polymers. *Journal of Applied Physics* 26(4): 359–362.
- Gaul, L., 1999. The influence of damping on waves and vibrations. *Mechanical Systems and Signal Processing* 13(1): 1–30.
- Gaul, L. & Schanz, M., 1999. A comparative study of three boundary element approaches to calculate the transient response of viscoelastic solids with unbounded domains. *Comput. Methods Appl. Mech. Engrg.* 179: 111–123.
- Gemant, A., 1936. A method of analyzing experimental results obtained from elasto-viscous bodies. *Physics* 7: 311–317.
- Gemant, A., 1938. On fractional differentials. *The Philosophical Magazine* 25: 540–549.
- Grünwald, A. K., 1867. Über ‘begrenzte’ Derivationen und deren Anwendung. *Zeitschrift für angewandte Mathematik und Physik* 12: 441–480.
- Koeller, R.C., 1984. Applications of fractional calculus to the theory of viscoelasticity. *Journal of Applied Mechanics* 51: 299–307.
- Lacroix, S., 1819. *Traité du calcul différentiel et du calcul intégral*. Paris: Courcier.
- Leibniz, G., 1962. *Leibnizsche Mathematische Schriften*. Georg Olm. Hildesheim.
- Liouville, J., 1832a. Mémoire sur le calcul des différentielles à indices quelconques. *J. Ecole Polytech.* 13: 71–162.
- Liouville, J., 1832b. Mémoire sur quelques questions de géométrie et de mécanique, et sur un nouveau genre de calcul pour résoudre ces questions. *J. Ecole Polytech.* 13: 1–69.
- Liouville, J., 1834. Mémoire sur le théoreme des fonctions complémentaires. *J. Reine Angew. Math.* 11: 1–19.
- Nutting, P. G., 1921. A new general law of deformation. *Journal of the Franklin Institute* 191: 679–685.
- Oldham, K. B. & Spanier, J., 1974. *The Fractional Calculus*. New York and London: Academic Press.
- Padovan, J., 1987. Computational algorithms for FE formulations involving fractional operators. *Computational Mechanics* 2: 271–287.
- Podlubny, I., 1999. *Fractional Differential Equations*. New York and London: Academic Press.
- Ross, B., 1975. A brief history and exposition of the fundamental theory of fractional calculus. In *Fractional Calculus and Its Applications, Lecture Notes in Mathematics 457*, Berlin: Springer-Verlag.
- Rouse, P.E.Jr., 1953. The theory of linear viscoelastic properties of dilute solutions of coiling polymers. *The Journal of Chemical Physics* 21(7): 1272–1280
- Schmidt, A., Oexl, S. & Gaul, L., 2000. Modellierung des viskoelastischen Materialverhaltens von Kunststoffen mit fraktionalem Zeitableitungen. In *18. CAD-FEM User’s Meeting 2000 – Internationale FEM-Technologietage; Proc intern. symp., Friedrichshafen, 20-22 September 2000*. Grafing: CAD-FEM GmbH
- Scott Blair, G. W. & Caffyn, J. E., 1949. An application of the theory of quasi-properties to the treatment of anomalous strain-stress relations. *The Philosophical Magazine* 40: 80–94.
- Zimm, B.H., 1956. Dynamics of polymer molecules in dilute solutions: viscoelasticity, flow birefringence and dielectric loss. *The Journal of Chemical Physics* 24(2): 269–278